

A COMPARATIVE INVESTIGATION OF A HIGH-VELOCITY IMPACT OF COSMIC BODIES UPON WATER AND GROUND

A. S. Smetannikov

UDC 533.6.01

The results of numerical simulation of the dynamics of a high-velocity impact upon a water surface are described in the approximation of two-dimensional hydrodynamics in cylindrical variables for bodies with dimensions, of about 1 km and impact velocities of about 50 km/sec. In the calculations a wide-range semiempirical equation of the state of water was used, with allowance for cold compression, phase transition into vapor, and the processes of dissociation and ionization. A comparison is made between calculations of an impact upon water and impacts upon different types of ground (gabbroid anorthosite, granite), which are described by both analytical equations of state and wide-range ones with phase transitions taken into account.

Investigations of the processes occurring on impact of space objects upon the surface in planets are of interest in geophysics and planetology and to date have undergone intensive development. The present work was carried out to elucidate the influence of the equations of state of the material upon which the impact occurs (target) on the dynamics of the flow induced. In considering a high-velocity impact upon water we assume that a semispace is filled with water. In reality, the depth of the ocean is finite; when a shock wave is reflected from the bottom, the material of the latter is entrained into motion, a bottom crater is being formed, the bottom may be uncovered, etc. [1], which will make a comparison with an impact upon a ground difficult. It is precisely to exclude the influence of these processes in comparing with an impact upon a ground in its "pure" form that such a statement of the problem has been used. We will consider the results of two-dimensional modeling of the dynamics of an impact of cosmic bodies upon a semispace filled with water and will compare it with similar modeling of an impact upon different types of ground (gabbroid anorthosite and granite).

To describe the flow set up upon impact of cosmic bodies upon a surface, a system of equations of gas dynamics for an axisymmetrical case in cylindrical coordinates r and z is employed:

$$\rho \left(\frac{\partial u}{\partial t} + v \frac{\partial u}{\partial r} + u \frac{\partial u}{\partial z} \right) = - \frac{\partial P}{\partial z}, \quad \rho \left(\frac{\partial v}{\partial t} + v \frac{\partial v}{\partial r} + u \frac{\partial v}{\partial z} \right) = - \frac{\partial P}{\partial r}, \quad (1)$$

$$\frac{1}{\rho} \frac{d\rho}{dt} = - \left[\frac{1}{r} \frac{\partial (rv)}{\partial r} + \frac{\partial u}{\partial z} \right], \quad \rho \frac{d\varepsilon}{dt} = - P \left[\frac{1}{r} \frac{\partial (rv)}{\partial r} + \frac{\partial u}{\partial z} \right].$$

For numerical solution of system (1) a fully conservative difference scheme is used with a coordinated approximation of flows in Euler variables [2]. In this scheme, the velocities are prescribed at the corners of cells, whereas energy, density, pressure, etc. are given at the centers. A description of the finite-difference scheme, the technique of solution, and the means of constructing a difference grid is given in [3].

In order to close the system of gasdynamic equations, it is necessary to prescribe the equations of state $P = P(\varepsilon, \rho)$ and $T = T(\varepsilon, \rho)$. At impact velocities on the order of 100 km/sec, the thermodynamic state of the material upon which the impact occurs changes in wide ranges — from a condensed one to a high-temperature plasma. In view of this, the equations of state must describe different phases of a substance and transitions between them, as well as take into account dissociation and ionization. Several such wide-range equations of the state of water are described in detail in the literature [4–8]. In order to calculate the equations of state of water, a procedure similar to that of [9, 10]

A. V. Luikov Heat and Mass Transfer Institute, National Academy of Sciences of Belarus, 15 P. Brovka Str., Minsk, 220072, Belarus. Translated from *Inzhenerno-Fizicheskii Zhurnal*, Vol. 80, No. 4, pp. 52–58, July–August, 2007. Original article submitted November 17, 2006.

was used. Pressure and energy are represented as the sum of the cold and thermal constituents, with the dissociation and ionization energies being additionally introduced into the energy term:

$$P = P_c + P_{th}, \quad \varepsilon = \varepsilon_c + \varepsilon_{th} + \varepsilon_d + \varepsilon_{ion}.$$

Expressions for the cold constituents of pressure and energy have the following form:

$$P_c = A (\delta^{\sigma+1} - \delta^{\mu+1}), \quad \varepsilon_c = \frac{A}{\rho_0} \left(\frac{\delta^\sigma}{\sigma} - \frac{\delta^\mu}{\mu} \right) + q,$$

where $\delta = \rho/\rho_0$; $\rho_0 = 1 \text{ kg/dm}^3$; $A = 0.5625 \text{ GPa}$; $\sigma = 4.2223$; $\mu = 0.2223$, and $q = 2.4 \text{ MJ/kg}$. These values differ somewhat from those given in [9] and conform better to both the dependence of the cold constituents on density according to [4, 6] and to the evaporation energy q in comparison with the experimental data on saturated steam.

The heat constituents at low temperature describe the molecular component (liquid and steam). Here, the heat capacity of the liquid is taken equal to $9R$ (a triatomic molecule) and of steam — $8/2R$ (eight degrees of freedom). The expression for the molecular component of energy is written as

$$\varepsilon_m = f_1(z) \frac{3k(T-T_0)}{2m}, \quad f_1(z) = \frac{2(3+4z)}{1+3z},$$

with $z = l\tau/\varphi^K$ taken as the parameter of interpolation between the indicated values of heat capacity, where $\tau = (T-T_0)/T_{cr}$, $\varphi = \rho/\rho_{cr}$ are the reduced temperature and density, K is a constant, and $T_0 = 273 \text{ K}$. The pressure in the indicated region of temperatures is defined as

$$P_m = f_2(z) \rho \varepsilon_m, \quad f_2(z) = \frac{3\gamma+z}{3+4z},$$

where γ is the Grüneisen coefficient of the liquid.

To perform an approximate account for the dissociation of molecules we assume that there is decomposition into two components, $2H + O$, with the dissociation energy $Q = 9.6 \text{ eV}$. Then the degree of dissociation β is found from the equation

$$\frac{\beta^2}{1-\beta} = \frac{C'}{\rho T^{1/2}} \exp(-Q/kT).$$

The value $C' = 10^7 \text{ (K}^{1/2}\cdot\text{kg)/m}^3$ is selected from comparison with the results of detailed calculations of the dissociation of a water molecule. The heat constituents of the energy and pressure of water with allowance for the dissociation of molecules into atoms are determined from the following expressions:

$$\varepsilon_{th} = (1-\beta) \varepsilon_m + 3\beta \varepsilon_a, \quad \varepsilon_a = \frac{3k(T-T_0)}{2m}, \quad \varepsilon_d = \beta kQ/m, \quad P_{th} = (1-\beta) P_m + 3\beta P_a, \quad P_a = \frac{2}{3} \rho \varepsilon_a.$$

On increase in the temperature, the ionization of atoms and formation of ions of different ionization stages are possible. Since the energy densities during the impact are very high, multiple ionization of ions was taken into account with the aid of the Saha system of equations (the index that prescribes the species of an atom is omitted for simplicity):

$$\frac{n_{i+1}n_e}{n_i} = 2 \frac{g_{i+1}}{g_i} \left(\frac{2\pi m_e kT}{h^2} \right)^{3/2} \exp\left(\frac{-I_{i+1}}{kT} \right), \quad \sum i n_i = n_e, \quad \sum n_i = n.$$

Then, when ionization is allowed for, the formulas for the thermal constituents of energy and pressure are modified as follows:

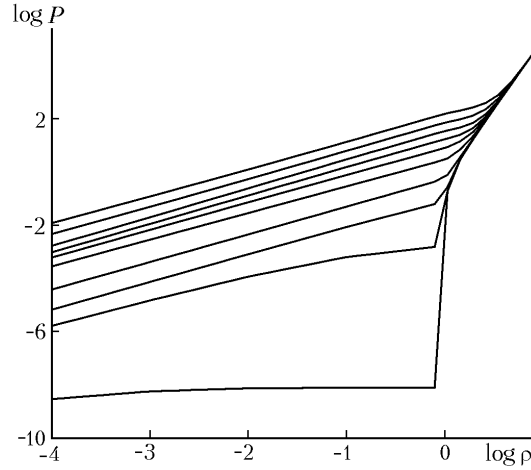


Fig. 1. Dependence of pressure on a set of energies according to wide-range equations of the state of water ($\log \epsilon$ changes from below upward from -0.5 to 2.5 with a step of 0.3333). ρ , kg/dm^3 ; P , GPa; ϵ , MJ/kg.

$$\epsilon_{\text{th}} = (1 - \beta) \epsilon_{\text{m}} + 3\beta (1 + x) \epsilon_{\text{a}}, \quad P_{\text{th}} = (1 - \beta) P_{\text{m}} + 3\beta (1 + x) P_{\text{a}},$$

where $x = n_e/n$ is the degree of ionization. The ionization energy is determined from the expression

$$\epsilon_{\text{ion}} = \sum Q_i \alpha_i / m, \quad Q_i = \sum_{k=1}^i I_k, \quad \alpha_i = n_i / n.$$

The semiempirical parameters needed for calculation have the following values: $l = 1.615$, $K = 3$, $\rho_{\text{cr}} = 0.318 \text{ kg/dm}^3$, $T_{\text{cr}} = 647 \text{ K}$, and $\gamma = 0.72$. The dependences of pressure on density that were calculated by this technique for a set of values of internal energy are given in Fig. 1.

Several variants of an impact of cosmic bodies consisting of ice and having a size from 0.2 to 1 km upon water with impact velocities 20 – 80 km/sec were calculated. As an example of calculation we will consider the following variant. An incident body is prescribed in the form of a cylinder with its length equal to the diameter $H = d = 1 \text{ km}$ and with density $\rho = 0.92 \text{ kg/dm}^3$. Its velocity $U = 50 \text{ km/sec}$ is directed normally to the water surface. Since the qualitative picture of flow is similar to that given by the calculations of an impact upon a ground, we will describe it only briefly. At the initial instant of time, the body comes in contact with the water surface and the pressure at the place of impact increases rapidly. Two shock waves arise: one travels through the body of the striker and vaporizes it and the other — through the target material, with the striker, when it penetrates into the target, creating a crater (bubble), its substance spreading over the surface of the crater formed. The shock wave propagating through the water rather rapidly acquires a shape close to a hemispherical one and further on grows in size, weakening gradually. As long as its intensity is rather high, the target material will evaporate, with the latter being ejected from the bubble (crater) into the atmosphere. The fields of density, pressure, and temperature are shown in Fig. 2 for three instants of time. At time $t = 0.3 \text{ sec}$, a shock wave in water reaches a depths of $z = 4.3 \text{ km}$, with its radial size being a little bit less than 3 km . A shock wave in a gas rises to a height of 5.5 km , with its radius attaining 3.2 km . The depth of the crater (bubble) comes up to 4 km , with its radius exceeding 2 km . The maximum of the temperature in the region near the crater amounts to about 5 eV , with 4 eV in the gaseous region. With time, the dimensions of the region involved in a flow increase and the maximal parameters in it gradually go down. By the instant of time $t = 2 \text{ sec}$, the shock wave in the gas rises to a height of 22 km , expanding to a radius of 8 km . The maximum pressure in it amounts to 160 kbar with a temperature of 1.6 eV . The shock wave in the ground reaches a depth of 10 km with 8 km in radius. The maximum pressure in it is equal to 6.6 kbar . The hot region from the crater ascends to a height of

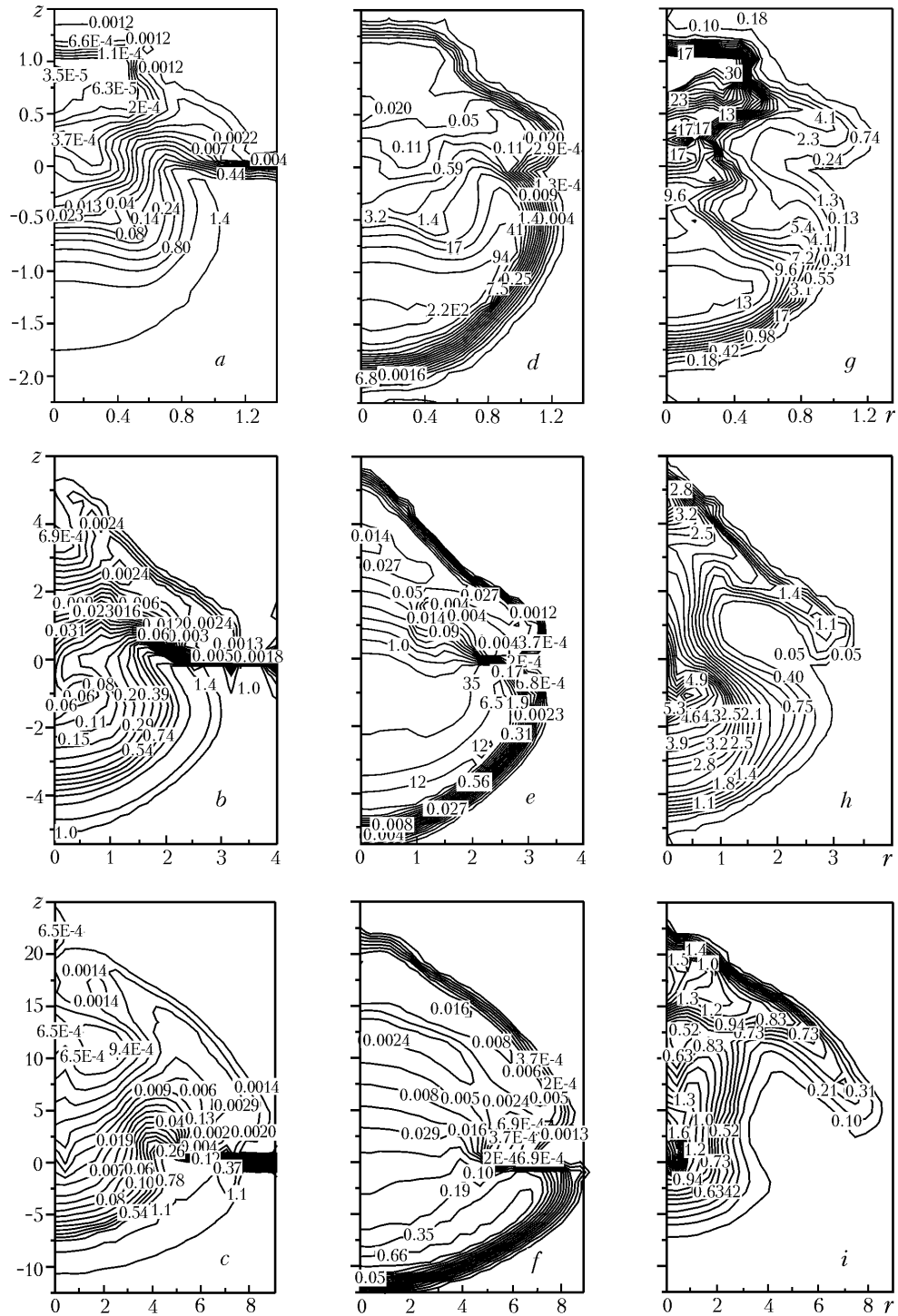


Fig. 2. Fields of density ρ (a–c), pressure P (d–f), and temperature T (g–i) at time moments 0.05 sec (a, d, g), 0.3 sec (b, e, h), and 2 sec (c, f, i). ρ , kg/dm^3 ; P , GPa; T , eV; z , r , km.

2.5 km, with the temperature maximum in the gas region reaching a height of 17.5 km. At that instant of time, the depth of the crater (bubble) is 7.5 km with a radius of 4 km.

The change in the integral characteristics with time is shown in Fig. 3. The asteroid is retarded, and its kinetic energy decreases rapidly; its internal energy increases and attains its maximum in $t = 0.18$ sec ($0.75/E_0$). There-

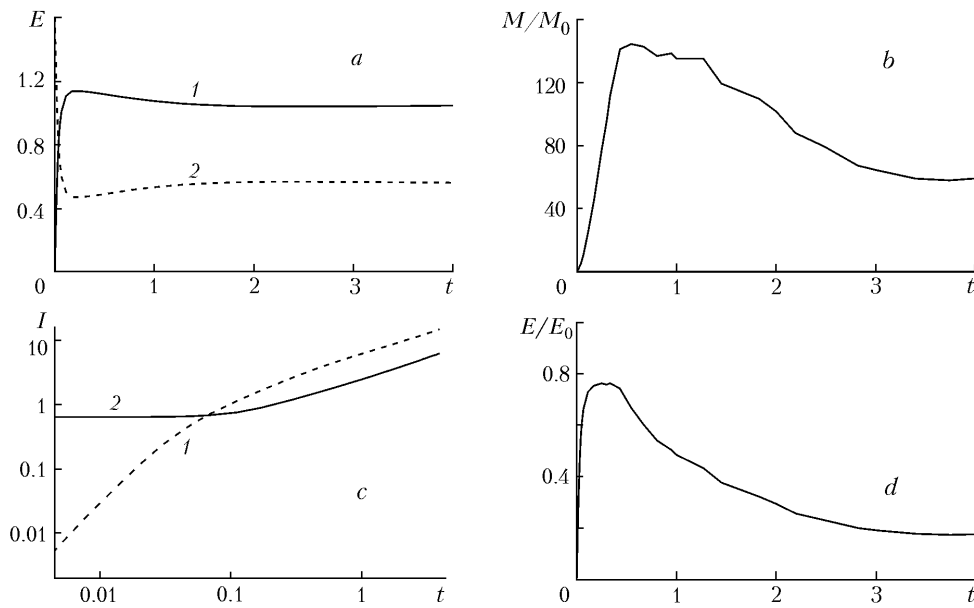


Fig. 3. Temporal behavior of integral characteristics: a) internal (1) and kinetic (2) energies; b) evaporated mass; c) radial (1) and basic (2) pulses; d) fraction of energy in evaporated substance. t , sec; E , 10^{20} J; I , 10^{19} , g-cm/sec.

after the internal energy gradually decreases (the kinetic energy increases) within 1.5 sec and thereupon remains practically constant. The axial and radial pulses increase with time and, starting from $t = 0.2$ sec, attain a self-similar dependence. The evaporated mass M_{evap} attains a maximum of $150M_0$ ($t = 0.5$ sec), changes little up to the moment $t = 1.4$ sec, and then decreases to $60M_0$ ($t = 3$ sec) and thereafter remains almost constant. The energy contained in the evaporated substance attains a maximum of $0.75E_0$ at the instant of time $t = 0.33$ sec and thereupon gradually decreases. To carry out estimations we adopt the energy of water evaporation equal to $q = 2.4$ MJ/kg. If the entire kinetic energy of the asteroid had been spent on evaporation, the maximum possible mass of evaporated water would be equal to $M'_{\text{evap}} = M_0 u^2 / (2q) = 500M_0$. Thus, the maximum of the ratio $M_{\text{evap}} / M'_{\text{evap}}$ is equal to 0.3. In the variant of calculation of impact upon a granite ground, that value is equal to 0.26, i.e., there is a small difference. A comparison of the energy maxima contained in the evaporated substance in these variants also demonstrated their closeness: 0.67 (granite) and 0.75 (water). We note that the moments when these maxima of the evaporated mass and energy were attained in the evaporated substance are also close for these two variants of calculation.

It is interesting to compare changes in the depths of craters with time for different types of target material and different impact velocities. For this we use the results of the following variants of two-dimensional calculations of an impact: upon gabbroid anorthosite with a velocity of $U = 17.7$ km/sec (variant 1), $U = 50$ km/sec (variant 2), $U = 141.4$ km/sec (variant 3); and with a velocity of $U = 50$ km/sec upon granite (variant 4) and water (variant 5). In all of the variants of calculation, the dimensions of the striker were the same ($H = d = 1$ km), with the materials of the striker and target coinciding. In the first three variants the Tillotson equation of state [4] was used; in the fourth variant it was a semiempirical wide-range equation of state with allowance for evaporation [4], and in the fifth variant — the aforegiven equation of state for water. As far back as in their earlier works on two-dimensional simulation of a high-velocity impact, Diens, and Walsh derived a similarity criterion [11] according to which a flow in a target at long times turns out to be identical if strikers are characterized by the same value LU^α with $\alpha \approx 0.59$. Here, $L = V^{1/3}$ is the characteristic size of the striker and U is the impact velocity. The long time signifies an interval much longer than the characteristic time $\tau = L/U$. The authors termed this concept the late-stage equivalence. According to this concept, the coordinate of the shock-wave front in the target X depends on time as follows:

$$X = Ct^{\frac{\alpha}{1+\alpha}} (LU^\alpha)^{\frac{1}{1+\alpha}} = C [L(Ut)^\alpha]^{\frac{1}{1+\alpha}}, \quad (2)$$

where C is the dimensionless constant. For the sake of definiteness, as X we select the position of the shock-wave front on the symmetry axis. The velocity of the shock-wave front is equal to

$$D = \frac{dX}{dt} = \frac{\alpha}{1+\alpha} \frac{X}{t} = \frac{\alpha}{(1+\alpha)} C \frac{1+\alpha}{\alpha} \left(\frac{LU^\alpha}{X} \right)^{\frac{1}{\alpha}} = \frac{\alpha}{(1+\alpha)} C \left(\frac{LU^\alpha}{t} \right)^{\frac{1}{1+\alpha}}. \quad (3)$$

The latter two equalities in (3) demonstrate the way in which the shock-wave velocity changes depending on the distance covered or with time. Since the pressure in the shock wave considerably exceeds the initial pressure in the target, the density at the shock-wave front attains a limiting compression ρ_1 which is proportional to the target density ρ_0 (for a perfect gas, $\rho_1 = \frac{\gamma+1}{\gamma-1} \rho_0$). Therefore, the pressure at the shock-wave front is proportional to the value

$$P \sim \rho_0 D^2 = \rho_0 \frac{\alpha^2}{(1+\alpha)^2} C^{\frac{2(1+\alpha)}{\alpha}} \left(\frac{L}{X} \right)^{\frac{2}{\alpha}} U^2 = \rho_0 \frac{\alpha^2 C^2}{(1+\alpha)^2} \left(\frac{L}{Ut} \right)^{\frac{2}{1+\alpha}} U^2. \quad (4)$$

Relation (4) demonstrates the similarity law for transition from some velocities to others. The pressure at the shock-wave front has a given value at distances proportional to LU^α or instants of time proportional to LU^α . Thus, the reduced coordinates (to compare different-velocity impacts) have the following dependence on the impact velocity:

$$X_1 \sim \frac{X}{LU^\alpha}, \quad t_1 \sim \frac{t}{LU^\alpha}. \quad (5)$$

These very dependences can be seen from expressions (3) for the shock-wave velocity. If we go over from the velocity to the kinetic energy of the striker $E \sim U^2$, we will obtain the following dependence of the reduced coordinates on energy: $X_1 \sim X/E^{\alpha/2}$ and $t_1 \sim t/E^{\alpha/2}$. As is known, in the self-similar solution of the problem on a spherical strong explosion (obtained by L. I. Sedov [12]) with energy E , these coordinates have the form $r \sim r/E^{1/3}$ and $t_1 \sim t_1/E^{1/3}$. Thus, the dependences of the reduced coordinates on the energy of impact and explosion differ not very markedly: for an impact ($\alpha = 0.59$) $E^{\alpha/2} = E^{1/3.4}$, whereas for an explosion $E^{1/3}$. In these coordinates, in the shock-wave-front motion law (2) the dependence on the impact velocity disappears (is transferred into the reduced coordinates):

$$X_1 = C_1 t_1^{\frac{\alpha}{1+\alpha}}, \quad (6)$$

where C_1 is a constant (dimensional). This relation allows one to compare different-velocity impacts by using a single relation.

To consider the change in the depth of the crater with time we will note the following. In the problem on motion of a gas under the action of a short impact (a one-dimensional approximation, plane geometry equation of state for a perfect gas) it was clearly shown by Ya. B. Zel'dovich that in a flow there is always a small mass of gas which "remembers" the conditions of the effect and is not described by a self-similar solution [13, 14]. It is significant that this gas region, which retreats from the target, is located behind a specific line (beyond the sphere of influence) and therefore does not exert any effect on the shock-wave propagation in the target. If such a picture is also correct for an axisymmetrical impact, then the flow in the crater (and also near its bottom) must be described by a self-similar solution. Then the reduced depth of the crater $h_1 \sim h/(LU^\alpha)$ vs. the reduced time (for long times) is described by a relation similar to (6):

$$h_1 = C_2 t_1^{\frac{\alpha}{1+\alpha}}. \quad (7)$$

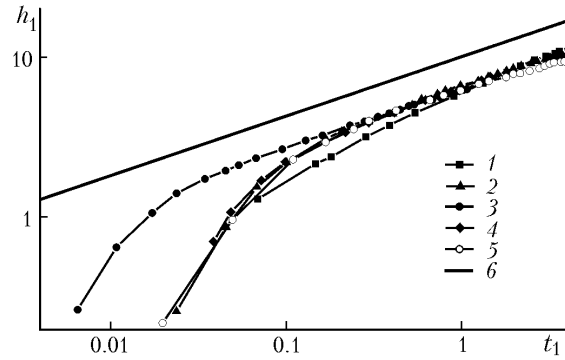


Fig. 4. Dependence of the reduced crater depth on reduced time. Curves 1–5 correspond to variants 1–5; 6) self-similar solution. h_1 , km; t_1 , sec.

Later a similar problem on a short impact was considered for condensed media described by the Mie–Grüneisen equation of state in [15], where also a self-similar solution was obtained with the self-similarity index changing within the range 0.61–0.63 (for various parameters of the equation of state for iron, copper, and aluminum).

Figure 4 demonstrates the calculated dependence of the depth of the crater on time (in reduced coordinates) for the above-indicated five variants. In this figure, as the reduced depth and time the values $h_1 = h / \left(\frac{U}{U_0} \right)^\alpha$ and $t_1 = t / \left(\frac{U}{U_0} \right)^\alpha$ are used at $\alpha = 0.59$ and $U_0 = 50$ km/sec. We note that calculations with different equations of state for the indicated variant yield somewhat different indices of self-similarity α lying within the range 0.58–0.63. It is also seen that for a time t exceeding approximately 10τ all the dependences attain a single self-similar line according to relation (7). For comparison, in the figure a bold line is given, which corresponds to the self-similar dependence with $\alpha = 0.59$ (it is displaced upwards not to obscure the results of two-dimensional calculations).

A comparison of impacts with the same velocity but different materials of the target allows the following conclusions. The values of the maximum of evaporated mass relative to the maximum possible evaporated mass turn out to be practically identical and equal to 0.26–0.3. The ratios of the maximum energy contained in the evaporated substance to the initial energy of the striker also appear to be close and approximately equal to 0.7. The dependence of the crater depth on time demonstrates the attainment of a single self-similar solution (at the late stage of the flow) for various materials of the target and in a wide range of impact velocities.

NOTATION

d , diameter of a body, km; D , velocity of a shock wave, km/sec; g_i and I_i , statistical sum and ionization potential of a corresponding ion; h , depth of a crater, km; \hbar , Planck constant; i , number of ion; k , Boltzmann constant; $L = V^{1/3}$, characteristic size of the striker, km; l , coefficient; V , volume of the striker, km^3 ; M_0 , mass of the striker, kg; m , mass of a molecule; m_e , mass of an electron; n_e and n_i , concentration of electrons and ions of i th multiplicity, m^{-3} ; P , pressure, GPa; Q , dissociation energy, J; q , evaporation energy, MJ/kg; r, z , coordinates, km; R , universal gas constant; t , time, sec; T , temperature, eV; v and u , radial and axial velocity components, km/sec; U , initial velocity of the striker, km/sec; α , self-similarity index; ε , energy of a unit mass, MJ/kg; ρ , density, kg/dm^3 ; ρ_0 , normal density of a substance in a condensed state, kg/dm^3 . Subscripts: e, electron; ion, ionization; c, cold; th, thermal; d, dissociation; cr, critical; m, molecular; a, atom; evap, evaporated.

REFERENCES

1. T. J. Ahrens and J. D. O'Keefe, Impact on the Earth, ocean and atmosphere, *Int. J. Impact Eng.*, **5**, 3–32 (1987).

2. V. M. Goloviznin, M. A. Ryazanov, A. A. Samarskii, O. S. Sorokovnikova, and S. Yu. Chernov, Difference schemes of gas dynamics with balanced convective flows, in: *Computational Methods in Mathematical Physics* [in Russian], MGU, Moscow (1986), pp. 5–41.
3. F. N. Borovik, G. S. Romanov, and A. S. Smetannikov, Modeling of the impact dynamics of large meteoric bodies on the surface of the planet, *Inzh.-Fiz. Zh.*, **72**, No. 4, 686–696 (1999).
4. B. V. Zamyshlyayev and M. G. Menzhulin, An interpolation equation of the state of water and steam, *Prikl. Mekh. Tekh. Fiz.*, No. 3, 113–118 (1971).
5. N. N. Kalitkin, L. V. Kuz'mina, and I. I. Sharipdzhanov, *Construction of the Equations of State of Chemical Compounds* [in Russian], Preprint No. 43 of the Institute of Applied Mathematics of the Academy of Sciences of the USSR, Moscow (1976).
6. S. V. Bobrovskii, V. M. Gogolev, M. G. Menzhulin, and R. V. Shilova, An interpolation thermodynamic model for water in the region of homogeneous and two-phase states, *Prikl. Mekh. Tekh. Fiz.*, No. 5, 130–139 (1978).
7. M. H. Rice and J. M. Walsh, Equation of state of water to 250 kilobars, *J. Chem. Phys.*, **26**, No. 4, 824–830 (1957).
8. A. M. Belyaev, V. S. Vorob'ev, and A. L. Khomkin, A wide-range equation of state of water, *Teplofiz. Vys. Temp.*, **28**, No. 3, 467–472 (1990).
9. S. N. Kolgatin, Simple interpolation equations of the state of nitrogen and water, *Zh. Tekh. Fiz.*, **64**, No. 7, 1–9 (1995).
10. S. N. Kolgatin and A. V. Khachatur'yants, Interpolation equations of the state of metals, *Teplofiz. Vys. Temp.*, **20**, No. 3, 447–451 (1982).
11. J. Dienes and J. Walsh, The theory of impact: Some general principles and method of calculation in Euler coordinates, in: *High-Velocity Impact Phenomena* [Russian translation], Nauka, Moscow (1973), pp. 48–111.
12. L. I. Sedov, *Similarity and Dimensionality Methods in Mechanics* [in Russian], Nauka, Moscow (1977).
13. Ya. B. Zel'dovich, Motion of a gas under the action of a short-duration pressure (shock), *Akust. Zh.*, **2**, 28–39 (1956).
14. Ya. B. Zel'dovich and Yu. P. Raizer, *Physics of Shock Waves and of High-Temperature Hydrodynamic Phenomena* [in Russian], Nauka, Moscow (1966).
15. S. I. Anisimov and V. A. Kravchenko, Shock wave in condensed matter generated by impulsive load, *Z. Naturforsch.*, **40a**, 8–13 (1985).